

## Perspectives for Detection of a Higgsino-like Relic Neutralino

A. Bottino<sup>a \*</sup>, N. Fornengo<sup>b,a</sup>, G. Mignola<sup>c,a †</sup>, M. Olechowski<sup>a ‡</sup>  
and S. Scopel<sup>d</sup>

<sup>a</sup> *Dipartimento di Fisica Teorica, Università di Torino and  
INFN, Sezione di Torino, Via P. Giuria 1, 10125 Turin, Italy*

<sup>b</sup> *Department of Physics and Astronomy, The Johns Hopkins University,  
Baltimore, Maryland 21218, USA.*

<sup>c</sup> *Theoretical Physics Division, CERN, CH-1211 Geneva 23, Switzerland*

<sup>d</sup> *Dipartimento di Fisica, Università di Genova and  
INFN, Sezione di Genova, Via Dodecaneso 33, 16146 Genoa, Italy*

### Abstract

It has been conjectured by Ambrosanio, Kane, Kribs, Martin and Mrenna (AKM) that the CDF event  $p\bar{p} \rightarrow e^+e^-\gamma\gamma E_T$  is due to a decay chain involving two neutralino states (the lightest and the next-to-lightest ones). The lightest neutralino ( $\chi_{AKM}$ ) has been further considered by Kane and Wells as a candidate for cold dark matter. In this paper we examine the properties of relic  $\chi_{AKM}$ 's in their full parameter space, and examine the perspectives for detection by comparing theoretical predictions to sensitivities of various experimental searches. We find that for most regions of the parameter space the detectability of a relic  $\chi_{AKM}$  would require quite substantial improvements in current experimental sensitivities. The measurements of neutrino fluxes from the center of the Earth and of an excess of  $\bar{p}/p$  in cosmic rays are shown to offer some favorable perspectives for investigating a region of the  $\chi_{AKM}$  parameter space around the maximal  $\tan\beta$  value allowed by the model.

---

\*E-mail: bottino@to.infn.it, fornengo@jhup.pha.jhu.edu, mignola@vxcern.cern.ch,  
Marek.Olechowski@Physik.TU-Muenchen.DE, scopel@ge.infn.it

†Present address: LAPP, Annecy, France

‡On leave of absence from the Institute of Theoretical Physics, Warsaw University, Poland.  
Present address: Physics Department, Technische Universität München, D-85748 Garching,  
Germany

## I. INTRODUCTION

The occurrence at CDF of the single event  $p\bar{p} \rightarrow e^+e^-\gamma\cancel{E}_T$  [1] has prompted two different supersymmetric interpretations [2–7], although also a non-supersymmetric explanation has been proposed [8].

The two supersymmetric interpretations have a common scheme to explain the CDF event: first, an  $\tilde{e}^+\tilde{e}^-$  pair is produced,  $p\bar{p} \rightarrow \tilde{e}^+\tilde{e}^-$ , then the following decay chain takes place  $\tilde{e}^\pm \rightarrow e^\pm\tilde{X}_2, \tilde{X}_2 \rightarrow \tilde{X}_1\gamma$ , where  $\tilde{X}_1$  and  $\tilde{X}_2$  are the lightest and the next-to-lightest supersymmetric particles (LSP and NLSP, respectively). The two supersymmetric interpretations differ in the identification of  $\tilde{X}_1$  and  $\tilde{X}_2$  with definite supersymmetric particles. In one interpretation [3,7]  $\tilde{X}_1$  and  $\tilde{X}_2$  are identified with the lightest and next-to-lightest neutralinos  $\chi_1$  and  $\chi_2$ , respectively; in the second interpretation [2–6]  $\tilde{X}_2$  is the lightest neutralino  $\chi_1$ , whereas  $\tilde{X}_1$  is identified with the gravitino, which has the role of the lightest supersymmetric particle.

To test whether or not one of the supersymmetric interpretations is correct, various possible processes which can occur at CERN LEP or at Fermilab Tevatron have been discussed in Refs. [2–7].

Furthermore, should one of the supersymmetric interpretations be valid, this would have implications for the presence of supersymmetric particles as relics in the Universe; these could also provide a substantial contribution to the cosmological matter density [9]. Thus the natural question arises, whether any of these fossil particles could be detected either directly or indirectly (or whether they are already excluded in force of the present experimental bounds).

The case of relic gravitinos would practically represent a hopeless situation for experimental investigation, since gravitino interactions are too weak to allow detection [10]. In models of gauge-mediated supersymmetry breaking (where the gravitino is the LSP) also the lightest messenger particle may be a viable dark matter candidate with a substantial relic abundance. This possibility has been recently investigated in Ref. [11]. We do not pursue the discussion of the gravitino case any further here.

Instead, in this paper we address the problem of the possible detection of relic neutralinos, whose specific properties are appropriate to a correct interpretation of the CDF event [9].

As discussed in Refs. [3,7], the interpretation of the CDF event in terms of the decay chain  $p\bar{p} \rightarrow \tilde{e}^+\tilde{e}^-, \tilde{e}^\pm \rightarrow e^\pm\chi_2, \chi_2 \rightarrow \chi_1\gamma$ , sets a number of very stringent constraints on the supersymmetric parameter space, and in particular on the nature of the neutralinos. These constraints, due to the kinematics of the event, and to the required sizes for the relevant cross section and decay branching ratios, imply that  $\chi_1$  and  $\chi_2$  are a very pure higgsino and a very pure photino, respectively. Detailed descriptions of the resulting supersymmetric parameter space are given in Ref. [7], and some of these results will also be reported here in the next section. For the moment, let us just anticipate some of the most prominent features of the model. The parameter  $\tan\beta$  is in the very low side (i.e.  $1 \lesssim \tan\beta \lesssim 3$ ) of its natural range:  $1 \lesssim \tan\beta \lesssim 50$ ; also, for the soft-breaking gaugino masses one has  $M_1 \simeq M_2$ , rather than the usual relationship  $M_1 \simeq M_2/2$ , motivated by unification assumption at  $M_{GUT}$  (definitions and conventions for the supersymmetric parameters are as in Ref. [12]). Furthermore, the kinematics of the CDF event (combined with the lower bound from LEP data) entails that  $m_{\chi_2} - m_{\chi_1} \gtrsim 30$  GeV and  $30$  GeV  $\lesssim m_{\chi_1} \lesssim 65$  GeV. In the following, a

neutralino eigenstate of the lightest mass,  $\chi_1$ , will be denoted by  $\chi_{AKM}$ , when its properties are those required by the supersymmetric interpretation of the CDF event, as suggested and described in Refs. [3,7] (LSP neutralino scenario).

In ref. [9] some properties of a  $\chi_{AKM}$  neutralino as a candidate for Cold Dark Matter (CDM) were discussed, and the perspectives for a direct detection were analysed, under the hypothesis that the contribution of  $\chi_{AKM}$  to the cosmological density  $\Omega$  is substantial. The analysis was pursued there in the extreme case of a pure higgsino composition and in general for a parameter space sizably narrower than the one allowed by the supersymmetric interpretation of the CDF event. In particular, it was concluded that the perspectives for a direct detection for this candidate are rather favorable.

In the present paper we reconsider the properties of  $\chi_{AKM}$  as a relic particle, by expanding the previous analysis in many instances [13]: i) we explicitly take into account a possible gaugino-higgsino mixing in  $\chi_{AKM}$ , which, although very tiny, might nevertheless have sizeable consequences in some processes for  $\tan \beta \simeq 3$ ; ii) we relax the requirement that  $\chi_{AKM}$  contributes to  $\Omega$  significantly, since we wish to fully explore the experimental chances to detect a relic  $\chi_{AKM}$ , even in the case it is not the main component of Cold Dark Matter (CDM); iii) we implement all the constraints from accelerators, including  $b \rightarrow s + \gamma$  and the new bounds implied by the LEP2 measurements [14]; iv) we examine what are the chances to detect relic  $\chi_{AKM}$ 's using various detection strategies (direct detection as well as indirect measurements: neutrinos from the Sun [15] and from the Earth and the antiproton/proton ratio in cosmic rays).

The motivations for the previous points are the following. On very general grounds one expects that a higgsino-like neutralino, such as  $\chi_{AKM}$ , provides a large relic abundance  $\Omega_\chi h^2$ , but has very little chances to be detectable. Indeed, a higgsino interacts with matter through spin-dependent effects, whereas the sensitivities of the experimental searches which are based on neutralino-matter scattering, however expected to substantially improve in the near future, will still remain for a while only at the level of the much larger coherent effects [16]. Thus the perspectives for detection of a relic  $\chi_{AKM}$  in the near future appear to be rather gloomy. Nevertheless, the conjecture of Refs. [3,7,9] is very challenging and potentially so much far-reaching, that it deserves a more careful analysis from the point of view of the actual perspectives of detectability.

Therefore we have undertaken the present analysis, with the aim of investigating the various circumstances which could provide some better perspectives for experimental exploration of at least some physical region allowed to  $\chi_{AKM}$ . This is why first, by taking into account the gaugino-higgsino mixing, even if small, we explore the possibility that coherent effects may help in providing direct and indirect detection rates with more substantial contributions than the ones due to the spin-dependent effects. Of course, this cannot occur for configurations with  $\tan \beta \simeq 1$ , but could happen for neutralino compositions at the upper side of the allowed range for  $\tan \beta$ , i.e.  $\tan \beta \simeq 3$ . Secondly, we have relaxed the constraint that  $\chi_{AKM}$  provides substantial relic abundance, which in itself sounds rather arbitrary and at the same time forces  $\chi_{AKM}$  to stay in a region of the parameter space where neutralino cross sections are automatically small. After all, should one be able to detect relic neutralinos compatible with the unique CDF event, this would already be a major breakthrough, even if these neutralinos do not provide a large  $\Omega$ ! Finally, apart from the more standard detection techniques for WIMPs (direct detection and detection of neutrinos from macro-

scopic bodies), also the antiproton/proton ratio in cosmic rays has been considered. Indeed, the  $\chi_{AKM}$  neutralino holds some features which could favor this kind of signal: a small mass and a very tiny (but not vanishing) mixing [17].

A few more comments are in order here. All experimental data have to be correctly implemented in shaping the allowed parameter space for  $\chi_{AKM}$ . Therefore we have taken into account the  $b \rightarrow s + \gamma$  process which is a very constraining bound to be implemented in any realistic model (it is not clear whether or not it was properly taken into account in the previous analyses of Refs. [9,15]). Furthermore we have included in our analysis the very recent data from LEP2 [14]. In the next section we show how these new results further constrain the parameter space of Refs. [3,7]. The bounds on the Higgs masses, which are important for our evaluation of the detection signals, are obtained from the experimental data of Refs. [18,19].

The scheme of this paper is as follows. In section 2 we define the supersymmetric parameter space and examine some general properties of  $\chi_{AKM}$ . In sections 3 and 4 we present our results for the  $\chi_{AKM}$  relic abundance and for its detection rates, respectively. Conclusions are finally reported in section 5.

## II. MODEL PARAMETER SPACE

Our parameter space has been modelled according to the one of Ref. [7]. It issues from the requirement that the CDF event is due to the process:  $p\bar{p} \rightarrow \tilde{e}^+\tilde{e}^-$ ,  $\tilde{e}^\pm \rightarrow e^\pm\chi_2$ ,  $\chi_2 \rightarrow \chi_1\gamma$ . We only consider the case of  $\tilde{e}_L$  production, which appears to be the favourite scheme among those suggested in Ref. [7].

The parameters are:  $M_1, M_2, \mu, \tan\beta, m_A$  (mass of the CP-even Higgs neutral boson),  $m_{\tilde{t}} = m_{\tilde{q}}$  (this is the common mass for sleptons and squarks, taken to be degenerate, with the exception of the left-handed selectron (of mass  $m_{\tilde{e}_L}$ ) and of the lightest stop (of mass  $m_{\tilde{t}_1}$ ) and  $\theta_{\tilde{t}}$  (mixing angle in the stop mass matrix).

Our analysis of the properties of a relic  $\chi_{AKM}$  has been performed by varying the supersymmetric parameters of a low-energy Minimal Supersymmetric extension of the Standard Model (MSSM) in the following ranges [7]:

region A

$$\begin{aligned}
1.05 &\leq \tan\beta \leq 1.5 \\
55 \text{ GeV} &\leq M_2 \leq 90 \text{ GeV} \\
0.8 &\leq M_2/M_1 \leq 1.2 \\
-70 \text{ GeV} &\leq \mu \leq -33 \text{ GeV} \\
75 \text{ GeV} &\leq m_{\tilde{e}_L} \leq 140 \text{ GeV} \\
m_A &= 60, 100, 200, 400 \text{ GeV} \\
m_{\tilde{q}} &= 250, 500, 1000 \text{ GeV} \\
150 \text{ GeV} &\leq m_{\tilde{t}_1} \leq m_{\tilde{q}} \\
-\pi/2 &\leq \theta_{\tilde{t}} \leq \pi/2
\end{aligned} \tag{1}$$

region B

$$\begin{aligned}
1.5 &\leq \tan\beta \leq 2.8 \\
40 \text{ GeV} &\leq M_2 \leq 130 \text{ GeV} \\
1.2 &\leq M_2/M_1 \leq 2 \\
-70 \text{ GeV} &\leq \mu \leq -33 \text{ GeV} \\
75 \text{ GeV} &\leq m_{\tilde{e}_L} \leq 140 \text{ GeV} \\
m_A &= 60, 100, 200, 400 \text{ GeV} \\
m_{\tilde{q}} &= 250, 500, 1000 \text{ GeV} \\
150 \text{ GeV} &\leq m_{\tilde{t}_1} \leq m_{\tilde{q}} \\
-\pi/2 &\leq \theta_{\tilde{t}} \leq \pi/2
\end{aligned} \tag{2}$$

In both cases  $m_{\tilde{e}_L}$  has been further required to satisfy the kinematical constraints among  $m_{\tilde{e}_L}$  and the neutralino mass eigenvalues [7].

As usual, any neutralino mass-eigenstate is written as a linear superposition

$$\chi_i = a_i \tilde{\gamma} + b_i \tilde{Z} + c_i \tilde{H}_s + d_i \tilde{H}_a \tag{3}$$

where  $\tilde{\gamma}, \tilde{Z}$  are the photino and zino states and  $\tilde{H}_s, \tilde{H}_a$  are defined by  $\tilde{H}_s = \sin\beta \tilde{H}_1^\circ + \cos\beta \tilde{H}_2^\circ$ ,  $\tilde{H}_a = \cos\beta \tilde{H}_1^\circ - \sin\beta \tilde{H}_2^\circ$ , in terms of the higgsino fields  $\tilde{H}_1^\circ, \tilde{H}_2^\circ$ , supersymmetric partners of the Higgs fields  $H_1^\circ, H_2^\circ$ , which provide masses to the down-type and up-type quarks, respectively.

The lightest neutralino state  $\chi_1$ , obtainable by varying the supersymmetric parameters in the regions A and B is what we define as a  $\chi_{AKM}$  neutralino. Its mass turns out to be confined in the range:  $30 \text{ GeV} \lesssim m_\chi \lesssim 65 \text{ GeV}$  (in region B the upper limit is about 60 GeV).

It is worth noticing here that in the previous analyses of relic  $\chi_{AKM}$ 's [9,15], only a restricted region of the parameter space ( $\tan\beta \simeq 1$ ) was considered, where higgsino purity in  $\chi_{AKM}$  is most pronounced. Also, in Refs. [9,15] only the lowest part of the neutralino mass range was considered,  $30 \text{ GeV} \leq m_\chi \leq 40 \text{ GeV}$ , in order to avoid the Z-pole (and possibly Higgs-poles) in the neutralino pair-annihilation cross section, where the evaluation of the neutralino relic density requires great care. In this paper we include in our discussion both region A and region B of supersymmetric parameters. We also consider the whole  $m_\chi$  range and discuss the effect on the detection signals of a careful calculation of the relic abundance over the poles of the neutralino-neutralino annihilation cross section.

On the other side, as previously mentioned, the new constraints from LEP2 [14] have been included. We show some effects of these constraints in Fig.1. This figure displays in the plane  $\mu - M_2$  those AKM configurations of regions A and B (see Eqs.(1,2)) which survive the  $b \rightarrow s + \gamma$  constraint. It turns out that some of them are already excluded by the new LEP data. The various curves denote the chargino isomass contours at fixed  $\tan\beta$  which correspond to the current LEP lower bound on the chargino mass [14]. For a given value of  $\tan\beta$ , the configurations on the right of the relevant line are disallowed. In particular, one sees that no AKM configuration survives for  $\tan\beta \gtrsim 2.6$ .

The composition of  $\chi_{AKM}$  is what establishes the size of the neutralino relic abundance and of the detection rates. This composition is shown in Fig.2. In Sect.a of this figure we give the values of the weights  $|a_1|^2, |b_1|^2, |c_1|^2, |d_1|^2$  of the  $\tilde{\gamma}, \tilde{Z}, \tilde{H}_s, \tilde{H}_a$  components for the

smallest value of  $\tan\beta$ :  $\tan\beta = 1.05$ . In Sect.b we display the values of the same quantities cumulatively for the two values  $\tan\beta = 2.15, 2.5$ . We notice that, as anticipated,  $\chi_{AKM}$  is largely dominated by  $H_s$ , with a next-to-leading contribution from  $\tilde{Z}$ . In Sect.c of Fig.2 we give a scatter plot for the fractional weights of these two main components of  $\chi_{AKM}$  over the full grid of Eqs.(1, 2). For some configurations of region B the value of the ratio  $|b_1|^2/|c_1|^2$ , even if small, may nevertheless be sizeable enough to allow coherent effects in neutralino-matter interaction to overcome the spin-dependent ones.

### III. RELIC ABUNDANCE OF $\chi_{AKM}$

The neutralino relic abundance  $\Omega_\chi h^2$  is evaluated using the standard formula

$$\Omega_\chi h^2 = 3.3 \times 10^{-38} \frac{1}{\sqrt{g_*(x_f)}} \frac{\text{cm}^2}{I(x_f)} \quad (4)$$

where

$$I(x_f) = \int_0^{x_f} dx \langle \sigma_{ann} v \rangle . \quad (5)$$

$\langle \sigma_{ann} v \rangle$  is the thermally-averaged annihilation cross section times the relative velocity,  $g_*(x_f)$  is the number of degrees of freedom at the freeze-out temperature  $T_f$  and  $x_f = T_f/m_\chi$ .

Whenever the neutralino-neutralino annihilation cross section is not in the proximity of a pole or when anyway a great accuracy in the estimate of  $\Omega_\chi h^2$  is not important, we simply expand  $\langle \sigma_{ann} v \rangle$  at small velocities  $\langle \sigma_{ann} v \rangle = a + bx$  ( $x = T/m_\chi$ ), and thus  $I(x_f) = ax_f + bx_f^2/2$  [20,21].

Otherwise, when we are close to a pole for the annihilation cross section and we require a careful evaluation for the relic abundance, the function  $I(x_f)$ , which entails multiple integrations over  $x$  and over the two particle velocities, is carefully evaluated, in part analytically and in part numerically [22,23]. Since this procedure is much computer-time consuming, we have applied the following selection criteria. Out of the full set of neutralino configurations explored through a scanning of the regions A and B, we have selected a number of configurations (denoted as set S in the following) which, according to our estimates of detection rates, have more chances to be detected in the future. The set S will be precisely defined later on. For the configurations of set S the relic abundance has been evaluated in the exact way (and compared to the approximated estimate), whereas for other configurations only the approximate method, based on the low-velocity expansion, has been adopted.

In the evaluation of  $\langle \sigma_{ann} v \rangle$  all the  $f\bar{f}$  final states as well as the complete set of Born diagrams have been taken into account [24].

In Fig.3 we display the results of our evaluation. Diamonds and crosses represent the values of  $\Omega_\chi h^2$  for configurations of set S (diamonds denote the values of  $\Omega_\chi h^2$  calculated in the exact way, crosses give the values obtained with the low-velocity approximation). Dots denote the values  $\Omega_\chi h^2$  for the other configurations (in the low-velocity approximation).

Some interesting features show up in this figure: i)  $\Omega_\chi h^2$  displays the typical dip at about 45 GeV (Z-pole); ii) in going through the pole in  $\sigma_{ann}$ , the approximated value of  $\Omega_\chi h^2$  changes from an overestimate to an underestimate of the correct value (see Sect.b of

Fig.3); iii) as expected, in region A ( $\tan\beta \simeq 1$ ) the relic abundance may be quite sizeable, and may even fall in the favorite range  $\Omega_{CDM}h^2 \simeq 0.2 \pm 0.1$  [25], whereas in region B it turns out to be systematically below 0.03.

The evaluation of  $\Omega_\chi h^2$  is important here not only to establish the role played by the  $\chi_{AKM}$  neutralino as a CDM candidate, but also to provide the value of the local (solar neighborhood) density  $\rho_\chi$ . This quantity enters in all the detection rates to be considered in the following. Here, to determine the value of  $\rho_\chi$ , we adopt the following rescaling recipe [26]. For each point of the parameter space, we take into account the relevant value of the cosmological neutralino relic density. When  $\Omega_\chi h^2$  is larger than a minimal  $(\Omega h^2)_{min}$ , compatible with observational data and with large-scale structure calculations, we simply put  $\rho_\chi = \rho_l$ . When  $\Omega_\chi h^2$  turns out to be less than  $(\Omega h^2)_{min}$ , and then the neutralino may only provide a fractional contribution  $\Omega_\chi h^2 / (\Omega h^2)_{min} \equiv \xi$  to  $\Omega h^2$ , we take  $\rho_\chi = \rho_l \xi$ . The value to be assigned to  $(\Omega h^2)_{min}$  is somewhat arbitrary, in the range  $0.03 \lesssim (\Omega h^2)_{min} \lesssim 0.2$ . In the present paper we have used  $(\Omega h^2)_{min} = 0.03$ . As far as the value of  $\rho_l$  is concerned, we have taken the representative value  $\rho_l = 0.5 \text{ GeV} \cdot \text{cm}^{-3}$ . This corresponds to the central value of a recent determination of  $\rho_l$ , based on a flattened dark matter distribution and microlensing data:  $\rho_l = 0.51^{+0.21}_{-0.17} \text{ GeV} \cdot \text{cm}^{-3}$  [27].

#### IV. DETECTION RATES FOR $\chi_{AKM}$

The most natural question to be asked now is whether there may be some chance to detect a relic neutralino with the properties of  $\chi_{AKM}$ . To provide an answer to this question we examine in detail three of the main methods for detecting relic particles (neutralinos in our case) [28]: i) direct detection, ii) detection of neutrinos from macroscopic bodies (Earth and Sun), iii) measurement of an excess of  $\bar{p}/p$  in cosmic rays, due to neutralino-neutralino annihilation in the halo.

As mentioned in the introduction, on very general grounds one expects that the interaction of the  $\chi_{AKM}$  neutralino with matter takes place through spin-dependent effects [9]. This is due to the fact that  $\chi_{AKM}$  is an almost pure higgsino, and then couples to quarks mainly through a  $Z$ -exchange. This is particularly true for configurations where  $\tan\beta \simeq 1$ . However, as shown in Fig. 2, for  $\chi_{AKM}$  compositions at the upper extreme of the allowed  $\tan\beta$  range, *i.e.*  $\tan\beta = 2.5$ , the higgsino-gaugino mixing parameter  $|b_1|^2/|c_1|^2$  can reach a level of  $\simeq 10\%$  and then may switch on some coherent effects through Higgs-mediated or squark-mediated processes. This effect may trigger an enhancement in direct detection rates as compared to a simple evaluation based on spin-dependent effects only. A second beneficial effect due to a mixing in  $\chi_{AKM}$  is that also the neutrino outcome from the Earth (typically increased by coherent effects) might be sizably enhanced.

A third detection method for  $\chi_{AKM}$  investigated in the present paper is the measurement of the antiproton component in cosmic rays. This experimental mean is very interesting, in view of the upcoming projects [29,30], which should substantially increase the number of measured antiprotons, bringing the present total number of about 30 to something of order 600 in a few-year time [30]. This remarkable increase in statistics should soon allow us to discriminate between a fast-varying spectrum of secondary antiprotons and a flat spectrum of antiprotons of exotic origin for kinetic energies in the range  $100 \text{ MeV} \lesssim T \lesssim$  a few

GeV. Also from the theoretical point of view the peculiarity of  $\chi_{AKM}$  offers some interesting features for the  $\bar{p}/p$  ratio (tiny higgsino-gaugino mixing and small mass).

Now let us define our set S of AKM configurations. This is a set of representative points within regions A and B which satisfy the following prerequisites: their predicted signals either for detection of neutrinos from Earth and Sun (at least one of these) or for detection of antiprotons in cosmic rays is within two orders of magnitude from the current value of the relevant experimental upper bound (at 90 % C.L.).

### A. Direct detection

Let us start our analysis of the detection methods from the most natural one: direct detection. This consists in the measurement of the energy released by a neutralino in its scattering off a nucleus in an appropriate detector, by using very different experimental techniques [28]. Some of the most recent experimental results are given in Refs. [31–35].

In general, it is expected that, in the neutralino-nucleus scattering, coherent effects, when allowed by the neutralino composition, overcome spin-dependent effects. When this is the case, then the best way to compare experimental data, which usually refer to a variety of nuclear compositions, is to convert the upper limits on the energy spectra into upper bounds on the neutralino-nucleon scalar cross section  $\sigma_{scalar}^{(n)}$ . This procedure is a model-independent one, i.e. it does not depend on the neutralino composition.

However, as previously discussed, for configurations of region A, the  $\chi_{AKM}$  is a neutralino with a high higgsino-purity and then its spin-dependent interactions with matter are important. Therefore for configurations of region A the previous procedure is not the most appropriate one and consequently we consider a rate rather than the neutralino-nucleon cross section. As far as configurations of region B are concerned, it turns out that the maximal signals are already slightly dominated by coherent effects. Therefore, for our comparison between predictions and experimental upper limits for configurations of region B we use both quantities: rates and cross sections.

For our evaluation of cross sections and rates for the process at hand, we used the method described in Refs. [36]. Our results are reported in Figs.4-5. In Fig.4 we display the predicted values of the rate  $R_{NaI}$  for the scattering of a neutralino off a NaI detector, integrated over the range  $3.75 \text{ KeV} \leq E_{ee} \leq 5.25 \text{ KeV}$ , where  $E_{ee}$  is the electron-equivalent energy. The reason for considering this quantity is that it provides one of the most stringent experimental upper bounds (for neutralinos interacting through spin-dependent effects and with a mass in the range  $40 \text{ GeV} \leq m_\chi \leq 75 \text{ GeV}$ ):  $R_{NaI}^{expt} \lesssim 1 \text{ event}/(\text{Kg day})$  [32]. From Fig.4 it is clear that all the predicted values for AKM configurations fall far below the current experimental bound (by more than two orders of magnitude for both regions, region B being slightly better than region A).

Fig.5 displays the scatter plot of the neutralino-nucleon cross-section times the rescaling factor  $\xi$  for configurations of region B only and compares these to the experimental upper bound. The experimental limit shown in this figure refers to an experiment using a Ge-detector [35]. This bound is somewhat more restrictive than the previous one from the NaI-detector, since now we start dealing with coherent effects and then we can optimize all experimental data to obtain the most stringent upper limit. Consequently, the maximal



predicted signal for some configurations turns out to be a little closer to the current limit, but however away by about two orders of magnitude. We notice that some increase in  $R_{NaI}$  and  $\xi\sigma_{scalar}^{(n)}$  is due to the refined evaluation of the neutralino relic abundance (see Figs. 4b-5).

## B. Neutrinos from the Earth and from the Sun

Let us turn now to the possible signals consisting of fluxes of up-going muons through a neutrino telescope generated by neutrinos produced by pair annihilations of neutralinos captured and accumulated inside the Earth and the Sun. The evaluation of the muon fluxes, which is a rather elaborate multistep process, has been performed here according to the procedure described in Ref. [37], to which we refer for details.

In order to conform to the experimental data which we use as upper limits, we consider here fluxes of up-going muons integrated over muon energies above 1 GeV. The flux from the Earth  $\Phi_{\mu}^{Earth}$  is also integrated over a cone of half aperture of  $30^{\circ}$  centered at the nadir, the one from the Sun  $\Phi_{\mu}^{Sun}$  is integrated over the whole possible outcome from the Sun, i.e. integrated over  $25^{\circ}$  around the Sun direction. We compare our evaluations to the Baksan upper limits:  $\Phi_{\mu}^{Earth} \leq 2.1 \times 10^{-14} \text{cm}^{-2}\text{s}^{-1}$  (90% C.L.),  $\Phi_{\mu}^{Sun} \leq 3.5 \times 10^{-14} \text{cm}^{-2}\text{s}^{-1}$  (90% C.L.) [38].

Our results are shown in Figs.6-7. We notice that for region A (Fig.6a) the maximal value of  $\Phi_{\mu}^{Sun}$ , provided only by very few configurations at  $m_{\chi} \simeq 65$  GeV, is  $\simeq 5 \times 10^{-15} \text{cm}^{-2}\text{s}^{-1}$ , anyway below the experimental upper bound roughly by a factor of 6. These configurations were disregarded in previous analyses [9,15]. Most of the other configurations give signals largely spread over more than three decades. When we move from region A to region B (Fig.6b),  $\Phi_{\mu}^{Sun}$  increases as expected, since coherent effects start playing some role in enhancing the neutralino capture rate by the Sun. Here a significant number of configurations have a predicted level of  $\Phi_{\mu}^{Sun}$  within an order of magnitude from the current experimental bound. For region B an even more favorable comparison between predictions and experimental sensitivity occurs for  $\Phi_{\mu}^{Earth}$  (Fig.7). Indeed, the maximal predicted value is away from the present experimental limit only by a factor 2. However, it is again apparent from Fig.7 that the predicted values for  $\Phi_{\mu}^{Earth}$  are spread over a very wide range of a few decades. As expected, the configurations with the highest values for the flux are those with a light Higgs boson A ( $m_A \simeq 100$  GeV) and some higgsino–zino mixing. The gap in between the two groups of configurations in Fig.7 is indeed due to the step in  $m_A$  used in our sampling of the parameter space.

We again notice that some increase in the level of the fluxes in Fig.6b and Fig.7 is due to the refined evaluation of the neutralino relic abundance. Furthermore it is worth noticing that some improvements in the comparison of the predicted values for  $\Phi_{\mu}^{Earth}$  and the experimental data may be obtained through a more refined analysis of the fluxes in terms of their angular distribution [39].

### C. $\bar{p}/p$ in cosmic rays

The annihilation of neutralinos in our halo may generate some amount of antiprotons in our Galaxy. A way of discriminating them, against the background due to the secondary antiprotons produced by primary cosmic particles with the interstellar medium, is to look at the  $\bar{p}/p$  spectrum as a function of the kinetic energy  $T$ . At small  $T$  the  $\bar{p}/p$  ratio due to secondaries increases quickly, as  $T$  increases, whereas the signal has a flat behaviour.

Measurements of anti-protons have been going on for quite a long time with some conflicting results [28]. More recent data [40,41] seem to follow the behaviour of secondaries as evaluated in Ref. [42]. However, a much higher statistics is required to find out whether or not there might be a signal of some exotic origin for antiprotons. This very intriguing problem should be settled in a few-year time, due to upcoming experiments [29,30] which are expected to collect a total of about 600 antiprotons [30].

We have evaluated the  $\bar{p}/p$  ratio in the following way: i) the antiproton spectrum, as due to the neutralino pair annihilation in the halo, has been calculated as in Ref. [17], ii) the proton spectrum has been taken from Ref. [43], iii) the propagation of the two fluxes has been evaluated using a leaky box model with an energy-dependent confinement time taken from Ref. [44], iv) the two spectra have been modulated by employing the procedure of Ref. [45] with the modulation parameter of Ref. [41] and then integrated over the range  $250 \text{ MeV} \leq T \leq 1000 \text{ MeV}$  to conform to the experimental characteristics of one of the most significant experimental data:  $\bar{p}/p = 3.14_{-1.9}^{+3.4} \times 10^{-5}$  for  $250 \text{ MeV} \leq T \leq 1000 \text{ MeV}$  [41]. To make the comparison of our predicted values with the experimental data more meaningful, we use in the following the value  $\bar{p}/p \leq 7.5 \times 10^{-5}$  as indicative of a 90 % C.L. limit for antiprotons of exotic origin.

We show our results in Fig.8. We notice that for a limited number of configurations in region B (Fig.8b) the predicted signal is rather close to the experimental value, but for many others the signals are away by orders of magnitude. The maximal predicted value for  $\bar{p}/p$  is below the upper limit by a factor 3-4. Again it turns out that the improvement in the calculation of  $\Omega_\chi h^2$  enhances the expected signal. In Fig.9 we give a scatter plot of  $\bar{p}/p$  versus  $\Phi_\mu^{Earth}$  to show how the same set of  $\chi_{AKM}$  configurations provide the maximal predicted values for both of these two quantities. Fig.10 shows where these configurations are located in the  $\mu - M_2$  plane.

## V. CONCLUSIONS

The conjecture that the CDF event  $p\bar{p} \rightarrow e^+e^-\gamma\gamma E_T$  is due to a decay chain involving two neutralino states (the lightest and the next-to-lightest ones) [3,7] is certainly very intriguing, although great caution is in order, because of the existence of a single event of this sort and of the non-uniqueness in its interpretation [2-8]. Nevertheless, the interpretation of the event suggested in Refs. [3,7], if correct, would have so much impact on particle physics, that any possible experimental verification of it should be carefully investigated. Obviously, accelerators are the most suitable means for this purpose.

Also the implications for relic supersymmetric neutralinos deserve much attention and experimental investigation. With this target in mind, we have extended the analyses of

Refs. [9,15] in many ways. We have explored a much wider region in the supersymmetric parameter space than previously done and we have examined a variety of different detection means. In such a challenging enterprise of searching for a relic particle the only winning strategy is the one of combining as many independent searches as possible.

Let us now summarize some of our results. We have considered three detection methods for relic neutralinos: i) direct detection, ii) detection of neutrinos from macroscopic bodies (Earth and Sun), iii) measurement of an excess of  $\bar{p}/p$  in cosmic rays, due to neutralino-neutralino annihilation in the halo. For all of these search techniques we have evaluated the relevant signals exploring the widest allowed parameter space of the  $\chi_{AKM}$  neutralino and we have compared our results to the current experimental bounds. In no case present experimental data are such to provide information on a relic  $\chi_{AKM}$ . All experimental methods require a substantial improvement in sensitivities before they may be capable of exploring some sizeable region of the  $\chi_{AKM}$  parameter space. In general, the most easily accessible region is the one corresponding to the values of  $\tan\beta$  close to the upper part of the AKM range  $1.05 \leq \tan\beta \leq 3$  and to the smallest values of  $m_A$ . Unfortunately, as discussed in Sect.2, the new LEP2 data already exclude the  $\chi_{AKM}$  configurations with  $\tan\beta \gtrsim 2.6$ .

For direct detection the most easily accessible part of the  $\chi_{AKM}$  parameter space requires a very significant experimental improvement in sensitivities of 2-3 orders of magnitude. We emphasize that our conclusion is based directly on consideration of neutralino-nucleon cross section, and then automatically takes into account the most stringent experimental measurements.

The measurement of fluxes of upgoing muons from the center of the Earth appears to be in a much better situation, since some configurations are away from the present upper bound by a factor of two. However, an improvement of at least one order of magnitude in sensitivity would be necessary for an exploration of a significant number of configurations. The most suitable detector for this job appears to be MACRO with a muon energy threshold of about 1 GeV, whereas large-area neutrino telescopes such as AMANDA and NESTOR would not have much chances because of a much higher energy threshold.

We have shown that some  $\chi_{AKM}$  configurations may provide an excess of  $\bar{p}/p$  in cosmic rays at a level that is away from the present measured value by a factor 3-4. This fact deserves much attention in view of the expected increase of statistics in the upcoming experiments in space.

However, a word of caution is in order here. All our evaluations of signals for configurations in region B are very sensitive to the value assigned to the parameter  $(\Omega_\chi h^2)_{min}$ , which enters in our rescaling of  $\rho_\chi$ . Here we have used  $(\Omega_\chi h^2)_{min} = 0.03$ , which roughly corresponds to a minimal value for  $(\Omega_\chi h^2)_{min}$ . If a larger value of  $(\Omega_\chi h^2)_{min} = f \times 0.03$  ( $f$  greater than one) is employed, then in region B the estimates for  $R$  and  $\Phi_\mu$  have to be reduced by a factor  $1/f$  and the values of  $\bar{p}/p$  by a factor  $(1/f)^2$ . The same considerations apply to those configurations of region A, whose relic abundance is smaller than  $(\Omega_\chi h^2)_{min}$ .

Finally, we point out that in the present paper our aim was to establish a comparison between the level of the maximal signals due to a  $\chi_{AKM}$  neutralino and the experimental sensitivities currently available or expected in a near future. It is obvious that, in view of an actual experimental measurement, specific signatures and signal to background discriminations should be carefully investigated. This is beyond the scope of the present analysis.

### Acknowledgements

We wish to thank Lars Bergström for interesting discussions. N. Fornengo gratefully acknowledges a post-doc fellowship of the Istituto Nazionale di Fisica Nucleare and G. Mignola one of the Università di Torino. M. Olechowski wishes to thank the support of the Polish Committee of Scientific Research and grant SFB-375-95 (research in astroparticle physics) of the Deutschen Forschungsgemeinschaft. Partial support was provided by the Theoretical Astroparticle Network under contract No. CHRX-CT93-0120. This work was also supported in part by the Research Funds of the Ministero dell'Università e della Ricerca Scientifica e Tecnologica.

## REFERENCES

- [1] See, for instance, L. Nodulman (CDF Collaboration), talk at the International Europhysics Conference on High Energy Physics, Brussels, July 1996
- [2] S. Dimopoulos, M. Dine, S. Raby and S. Thomas, *Phys. Rev. Lett.* **76** (1996) 3494.
- [3] S. Ambrosanio, G.L. Kane, G.D. Kribs, S. Martin and S. Mrenna, *Phys. Rev. Lett.* **76** (1996) 3498.
- [4] S. Dimopoulos, S. Thomas and J.D. Wells, *Phys. Rev.* **D54** (1996) 3283.
- [5] J.L. Lopez and D.V. Nanopoulos, hep-ph/9607220
- [6] J. Hisano, K. Tobe and T. Yanagida, hep-ph/9607234
- [7] S. Ambrosanio, G.L. Kane, G.D. Kribs, S. Martin and S. Mrenna, hep-ph/9607414
- [8] G. Bhattacharyya and R. Mohapatra, *Phys. Rev.* **D54** (1996) 4204.
- [9] G.L. Kane and J.D. Wells, *Phys. Rev. Lett.* **76** (1996) 4458.
- [10] P. Fayet, *Phys. Lett.* **B86** (1979) 272.
- [11] S. Dimopoulos, G.F. Giudice and A. Pomarol, hep-ph/9607225
- [12] H.E. Haber and G.L. Kane, *Phys. Rep.* **117** (1995) 75.
- [13] Preliminary results of the present analysis were presented by A. Bottino, invited talk at the International Workshop "The Identification of Dark Matter", Sheffield University, September 7-11, 1996 (to appear in the Proceedings)
- [14] OPAL Collaboration, CERN Preprint CERN-PPE/96 October 4, 1996; M. Martinez, W. De Boer, M. Pohl, A.T. Watson representing the ALEPH, DELPHI, L3 and OPAL Collaborations, joint seminar at CERN, October 8, 1996
- [15] Signals from the Sun and direct detection for a restricted parameter space and under the assumption of sizeable contribution to  $\Omega$  are also considered in K. Freese and M. Kamionkowski, hep-ph/9609370
- [16] These considerations apply to direct detection and to detection of neutrinos from the center of the Earth. The low-flux signals of neutrinos from the Sun which are related to spin-dependent effects will only be accessible to large area neutrino telescopes (AMANDA, NESTOR) whose threshold energy will however be too high to allow detection of  $\chi_{AKM}$ .
- [17] A. Bottino, C. Favero, N. Fornengo and G. Mignola, *Astroparticle Physics* **3** (1995) 77.
- [18] ALEPH Collaboration, contribution to the International Europhysics Conference on High Energy Physics, Brussels, Belgium, July 1995 (Proc., to be published).
- [19] E. Accomando et al., CERN Yellow report, CERN-96-01, p. 351.
- [20] J. Ellis, J.S. Hagelin, D.V. Nanopoulos, K. Olive and M. Srednicki, *Nucl. Phys.* **B238** (1984) 453.
- [21] M. Srednicki, R. Watkins and K. Olive, *Nucl. Phys.* **B310** (1988) 693.
- [22] K. Griest and D. Seckel, *Phys. Rev.* **D43** (1991) 3191.
- [23] P. Gondolo and G. Gelmini, *Nucl. Phys.* **B360** (1991) 145.
- [24] A. Bottino, V. de Alfaro, N. Fornengo, G. Mignola and M. Pignone, *Astroparticle Physics* **2** (1994) 67.
- [25] V. Berezhinsky, A. Bottino, J. Ellis, N. Fornengo, G. Mignola and S. Scopel, *Astroparticle Physics* **5** (1996) 1.
- [26] T.K. Gaisser, G. Steigman and S. Tilav, *Phys. Rev.* **D34** (1986) 2206.
- [27] E.I. Gates, G. Gyuk and M. Turner, *Ap.J.* **449** (1995) L123.

- [28] For an exhaustive list of references on detection methods for neutralinos see: G. Jungman, M. Kamionkowski and K. Griest, *Phys. Rep.* **267** (1996) 195.
- [29] O. Adriani et al., *The magnetic spectrometer PAMELA for the study of cosmic anti-matter in space*, XXIV International Cosmic Ray Conference, OG 10.3.7, v.3, p.591, Roma, 1995
- [30] AMS Collaboration :1994, Alpha Magnetic Spectrometer for Extraterrestrial Study of Antimatter, Matter and Missing Matter on the International Space Station Alpha, Proposal.
- [31] M. Beck et al. (Heidelberg-Moscow), *Phys. Lett.* **B336** (1994) 141.
- [32] P.F. Smith et al., *Phys. Lett.* **B379** (1996) 299.
- [33] P. Belli et al., *Nucl. Phys. B* (Proc. Suppl.) **48** (1996) 60; R. Bernabei, invited talk at the International Workshop "The Identification of Dark Matter", Sheffield University, September 7-11, 1996 (to appear in the Proceedings).
- [34] A. Alessandrello et al., *Phys. Lett.* **B384** (1996) 316.
- [35] A.K. Drukier et al., *Nucl. Phys. A* (Proc. Suppl.) **28** (1992) 293.
- [36] A. Bottino, V. de Alfaro, N. Fornengo, G. Mignola and S. Scopel, *Astroparticle Physics* **2** (1994) 77.
- [37] A. Bottino, N. Fornengo, G. Mignola and L. Moscoso, *Astroparticle Physics* **3** (1995) 65.
- [38] M.M. Boliev et al. (Baksan Underground Telescope), *Nucl. Phys. B* (Proc. Suppl.) **48** (1996) 83.
- [39] An analysis along these lines is in progress, using new data from the MACRO detector and specific windows in the angular distribution of the upgoing muons (T. Montaruli, private communication and contribution to *Aspects of Dark Matter in Astro- and Particle Physics*, Heidelberg, September 1996 (to appear in the Proceedings)).
- [40] M. Hof et al. preprint LNF-96-010-p February 1996.
- [41] J.W. Mitchell et al., *Phys. Rev. Lett.* **76** (1996) 3057.
- [42] T.K. Gaisser and R.K. Schaefer, *Ap.J.* **394** (1992) 174.
- [43] M.J. Ryan, J.F. Ormes and V.K. Balasubrahmayan, *Phys. Rev. Lett.* **28** (1972) 985.
- [44] P. Chardonnet, G. Mignola, P. Salati and R. Taillet, *Phys. Lett.* **B384** (1996) 161.
- [45] J.S. Perko, *Astron. Astrophys.* **184** (1987) 119.

## Figure Captions

**Figure 1** – AKM configurations of regions  $A$  and  $B$  (see Eqs.(1,2)) which survive the  $b \rightarrow s + \gamma$  constraint, displayed in the plane  $\mu - M_2$ . The various curves denote the chargino isomass contours which correspond to the current LEP lower bound on the chargino mass [14], for different values of  $\tan \beta$ :  $\tan \beta = 1.05$  (solid),  $\tan \beta = 1.5$  (dotted),  $\tan \beta = 2.6$  (dot-dashed),  $\tan \beta = 2.8$  (dashed). Dots (circles) denote configurations of region A (B).

**Figure 2** – Sect.a displays the values of the weights  $|a_1|^2, |b_1|^2, |c_1|^2, |d_1|^2$  of the  $\tilde{\gamma}, \tilde{Z}, \tilde{H}_s, \tilde{H}_a$  components for the smallest value of  $\tan \beta$ :  $\tan \beta = 1.05$ . Sect.b shows the values of the same quantities cumulatively for the values  $\tan \beta = 2.15, 2.5$ . Sect.c shows a scatter plot for the fractional weights of the two main components of  $\chi_{AKM}$  over the full grid of Eqs.(1, 2).

**Figure 3** – Values of  $\Omega_\chi h^2$  for configurations in region A (B) are given in Sect.a (b). Diamonds and crosses represent the values of  $\Omega_\chi h^2$  for configurations of set S (diamonds denote the values of  $\Omega_\chi h^2$  calculated in the exact way, crosses give the values obtained with the low-velocity approximation). Dots denote the values  $\Omega_\chi h^2$  for the other configurations (in the low-velocity approximation only). The horizontal line corresponds to the value  $\Omega_\chi h^2 = 0.03$ , below which we apply rescaling for the local neutralino density.

**Figure 4** – Predicted values of the rate  $R_{NaI}$  for the scattering of a neutralino off a NaI detector, integrated over the range  $3.75 \text{ KeV} \leq E_{ee} \leq 5.25 \text{ KeV}$ , where  $E_{ee}$  is the electron-equivalent energy. Configurations in region A (B) are given in Sect.a (b). Diamonds and crosses denote the values of the displayed signal for configurations of set S when  $\Omega_\chi h^2$  is calculated with the exact expression and with the low-velocity approximation, respectively. Dots denote the values of the displayed signal for the other configurations, calculated in the low-velocity approximation only.

**Figure 5** – Scatter plot of the neutralino-nucleon scalar cross-section times the rescaling factor  $\xi$  for configurations of region B. The line denotes the upper bound on the cross-section obtained using the experimental results of Ref. [35] (Ge-detector). Diamonds, crosses and dots are as in Fig. 4.

**Figure 6** – The flux  $\Phi_\mu^{Sun}$  for configurations in region A (B) is given in Sect.a (b). Diamonds, crosses and dots are as in Fig.4. The horizontal line denotes the Baksan upper limit:  $\Phi_\mu^{Sun} \leq 3.5 \times 10^{-14} \text{ cm}^{-2} \text{ s}^{-1} (90\% C.L.)$  [38].

**Figure 7** – The flux  $\Phi_{\mu}^{Earth}$  for configurations in region B. Diamonds, crosses and dots are as in Fig.4. The horizontal line denotes the Baksan upper limit:  $\Phi_{\mu}^{Earth} \leq 2.1 \times 10^{-14} \text{cm}^{-2} \text{s}^{-1} (90\% C.L.)$  [38].

**Figure 8** –  $\bar{p}/p$  ratio in cosmic rays due to neutralino-neutralino annihilation in the galactic halo. The energy integration range is given in the text. The scatter plot refers to configurations of region A (B) in Sect. a (b). The horizontal line corresponds to the 90 % C.L. bound:  $\bar{p}/p \leq 7.5 \times 10^{-5}$ . Diamonds, crosses and dots are as in Fig.4.

**Figure 9** –  $\bar{p}/p$  versus  $\Phi_{\mu}^{Earth}$  for configurations of region B. Diamonds, crosses and dots are as in Fig.4. The horizontal line corresponds to the 90 % C.L. bound:  $\bar{p}/p \leq 7.5 \times 10^{-5}$ , the vertical line denotes the Baksan upper limit:  $\Phi_{\mu}^{Earth} \leq 2.1 \times 10^{-14} \text{cm}^{-2} \text{s}^{-1} (90\% C.L.)$ .

**Figure 10** – Location of the configurations of set S in the plane  $\mu - M_2$ . The curves are denoted as in Fig.1. Diamonds denote the configurations of set S, dots the other allowed configurations.



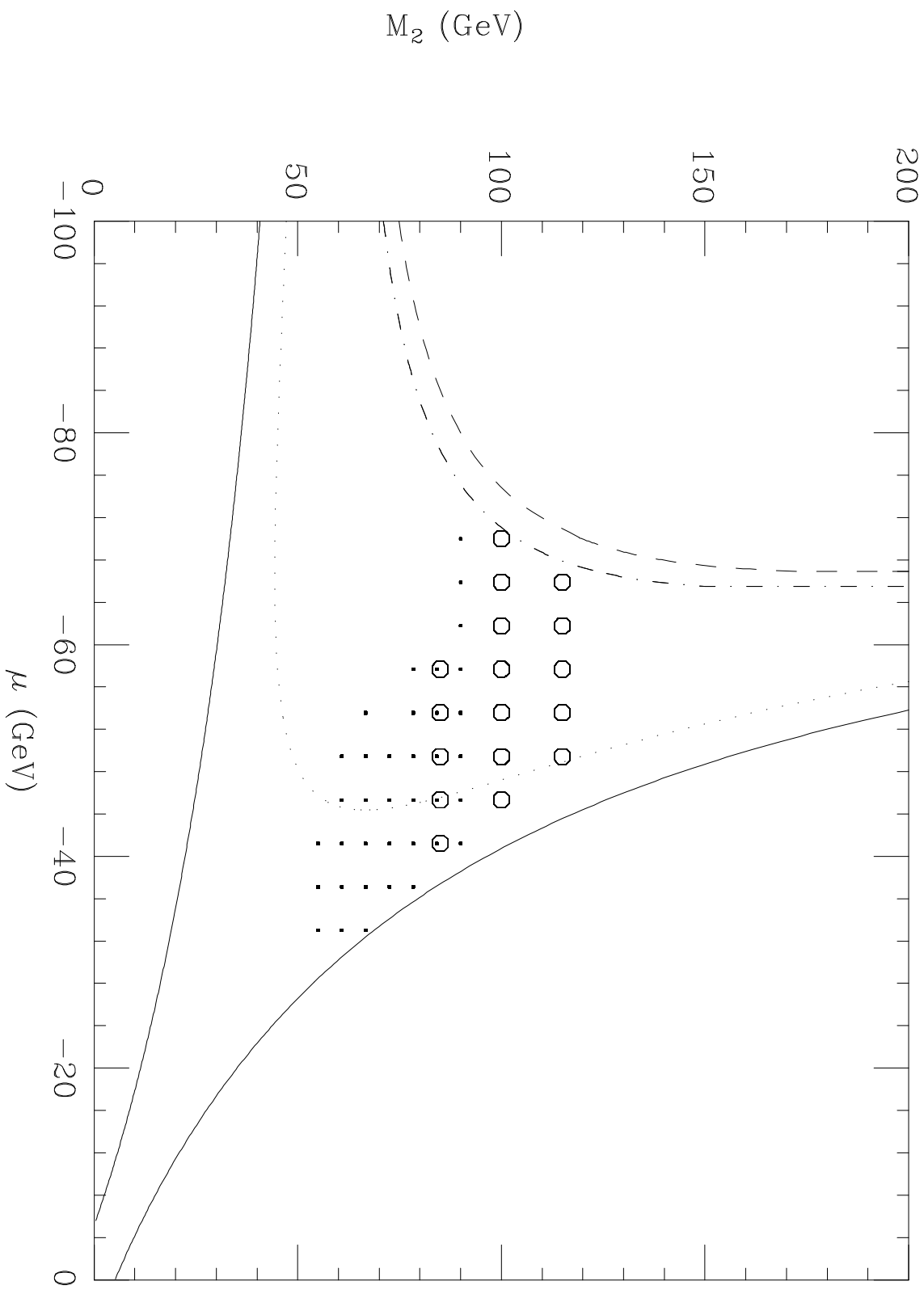
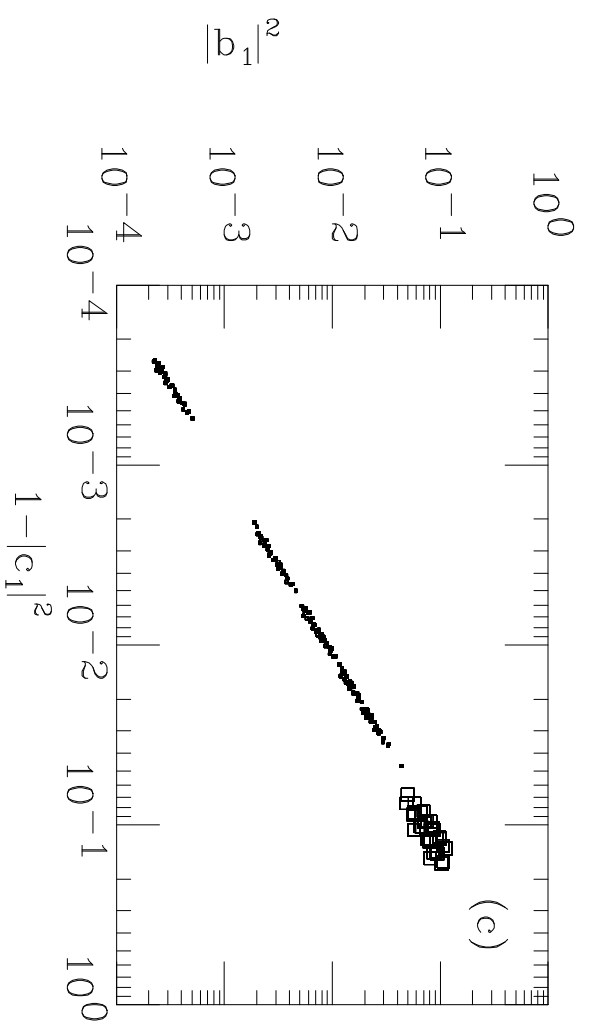
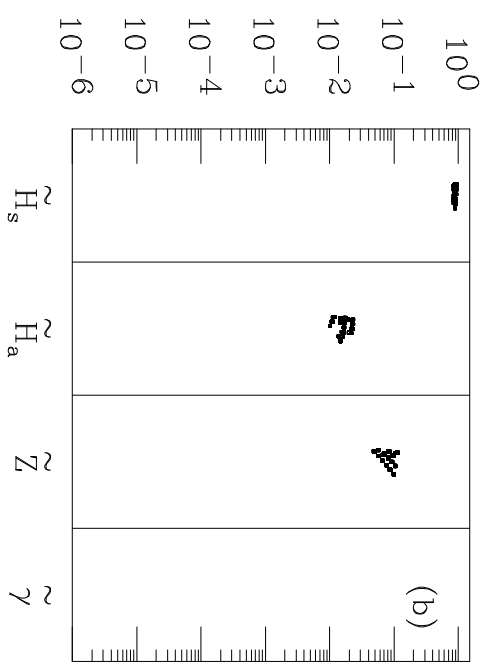
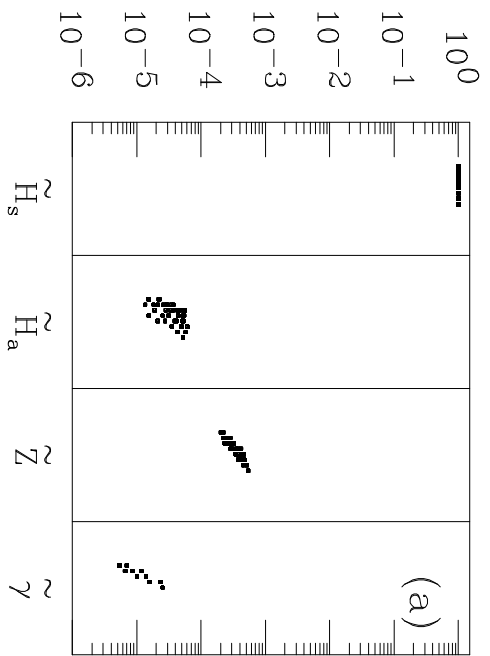


Figure 1



· Region A  
 □ Region B

Figure 2

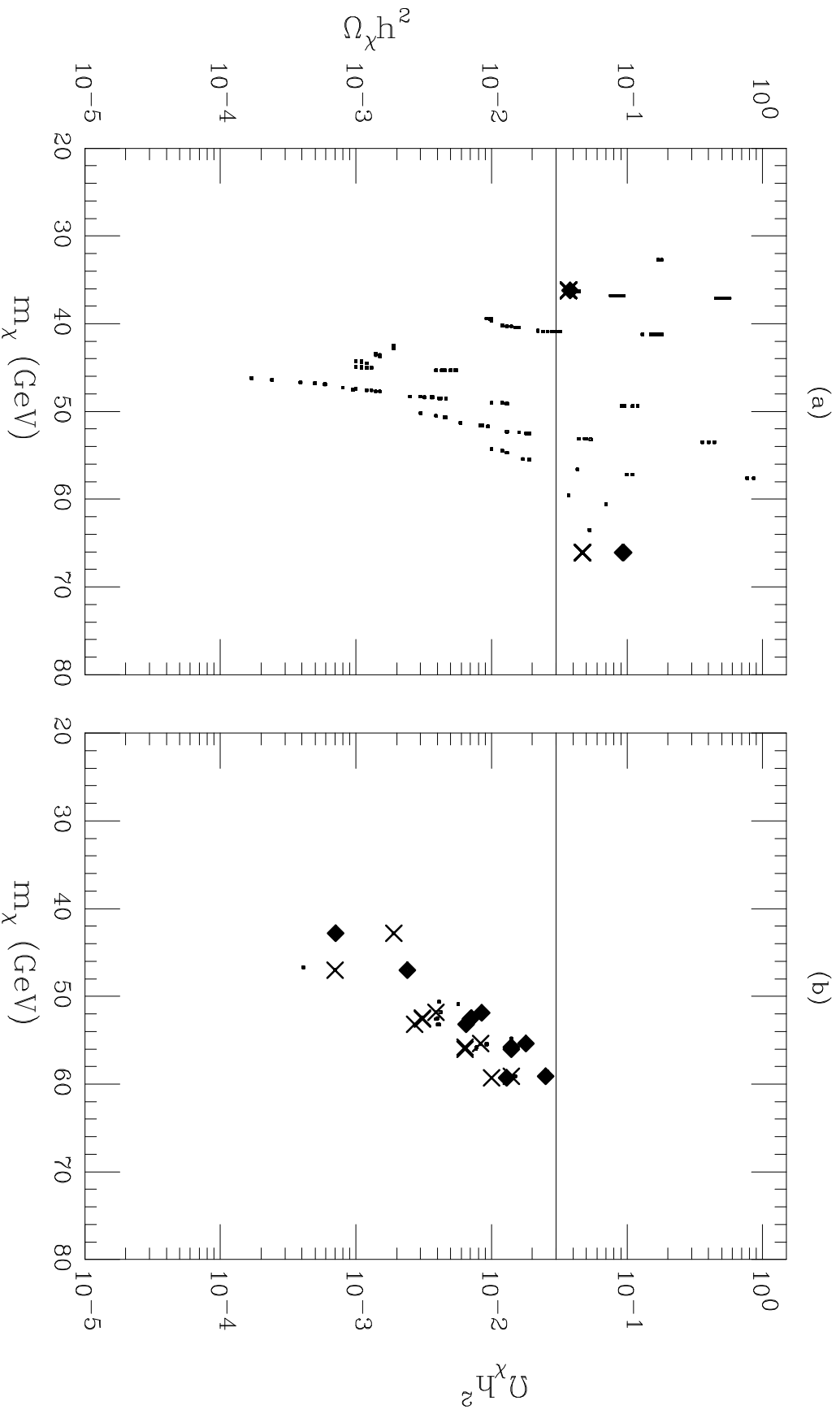


Figure 3

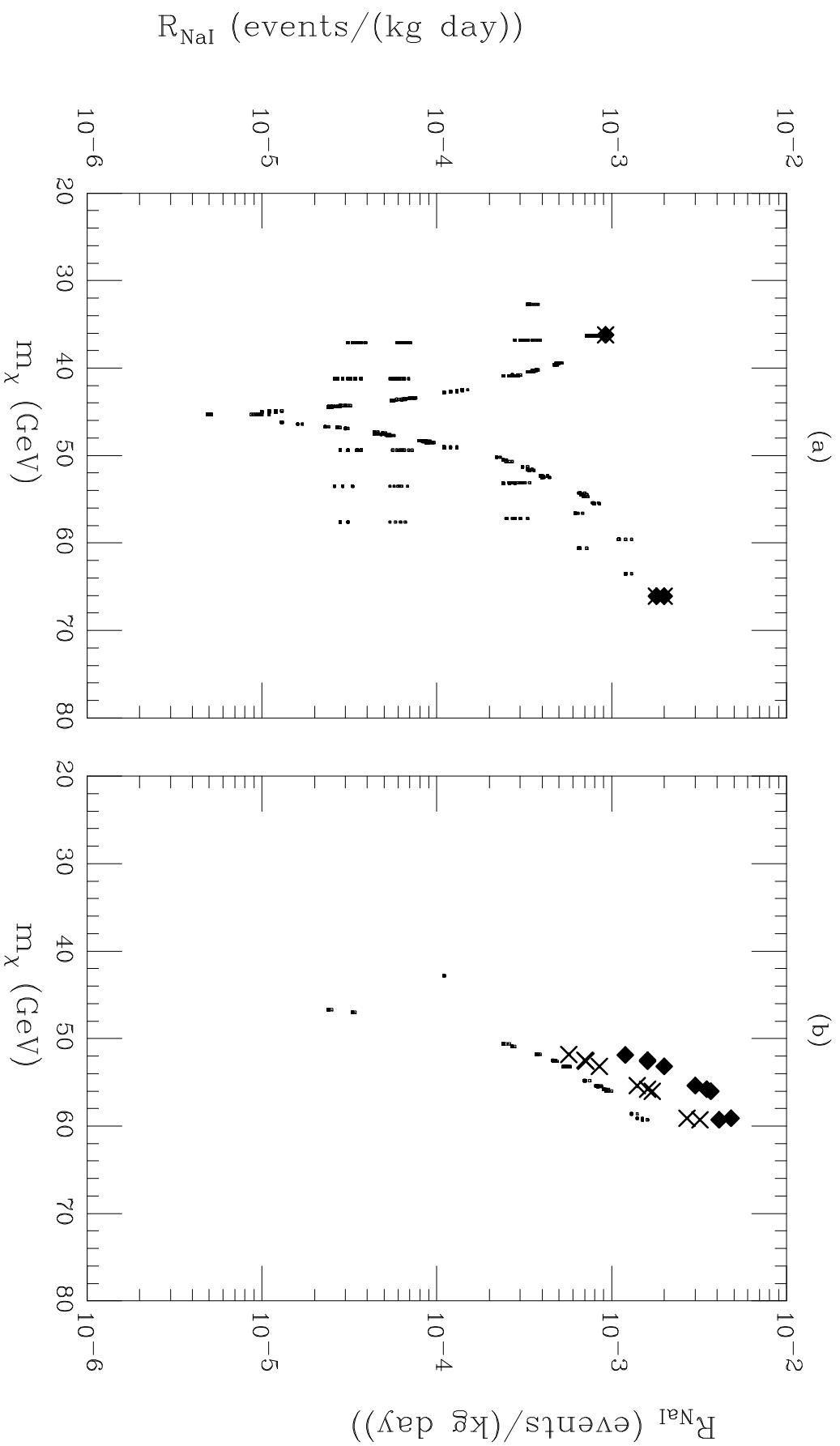


Figure 4

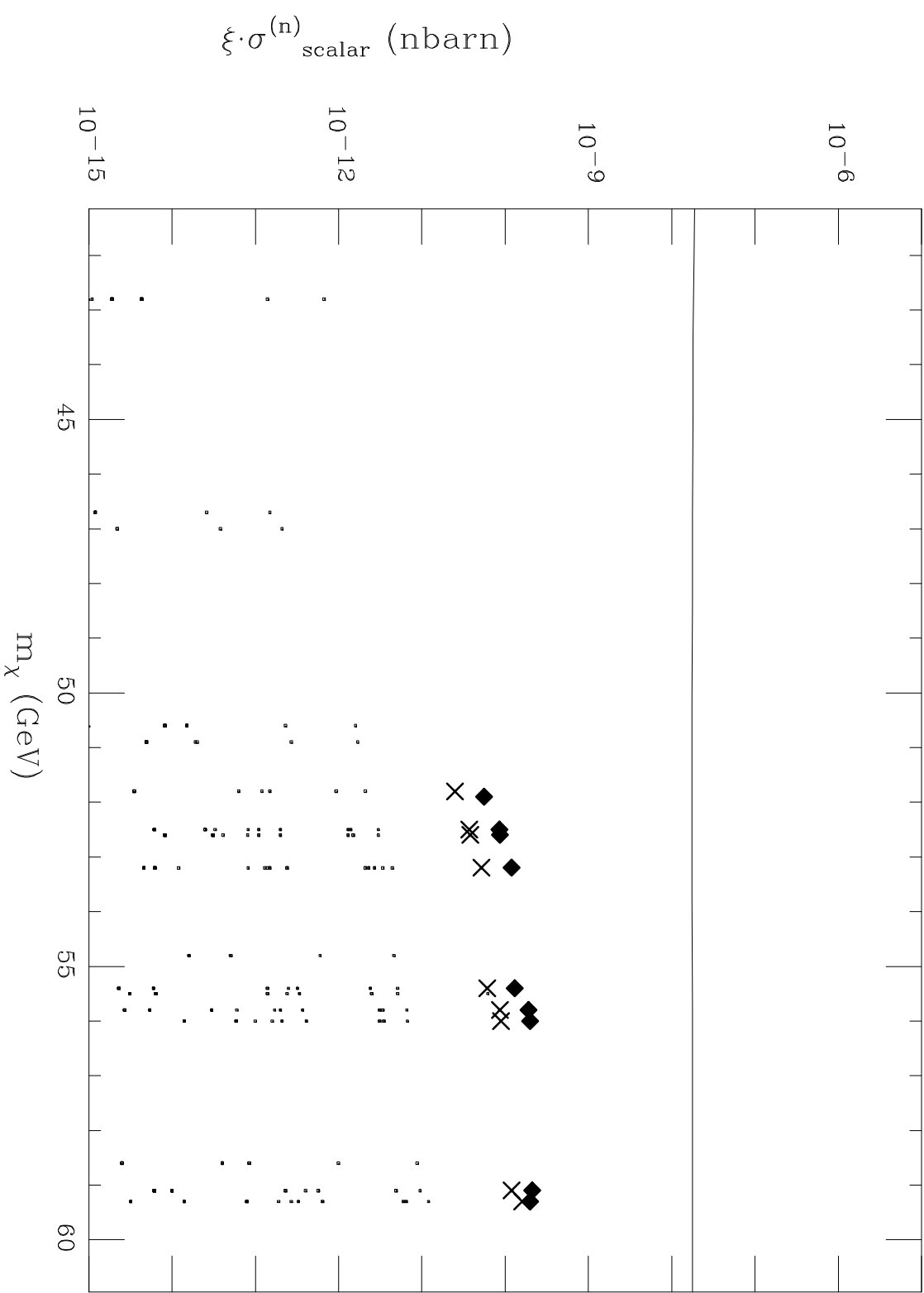


Figure 5

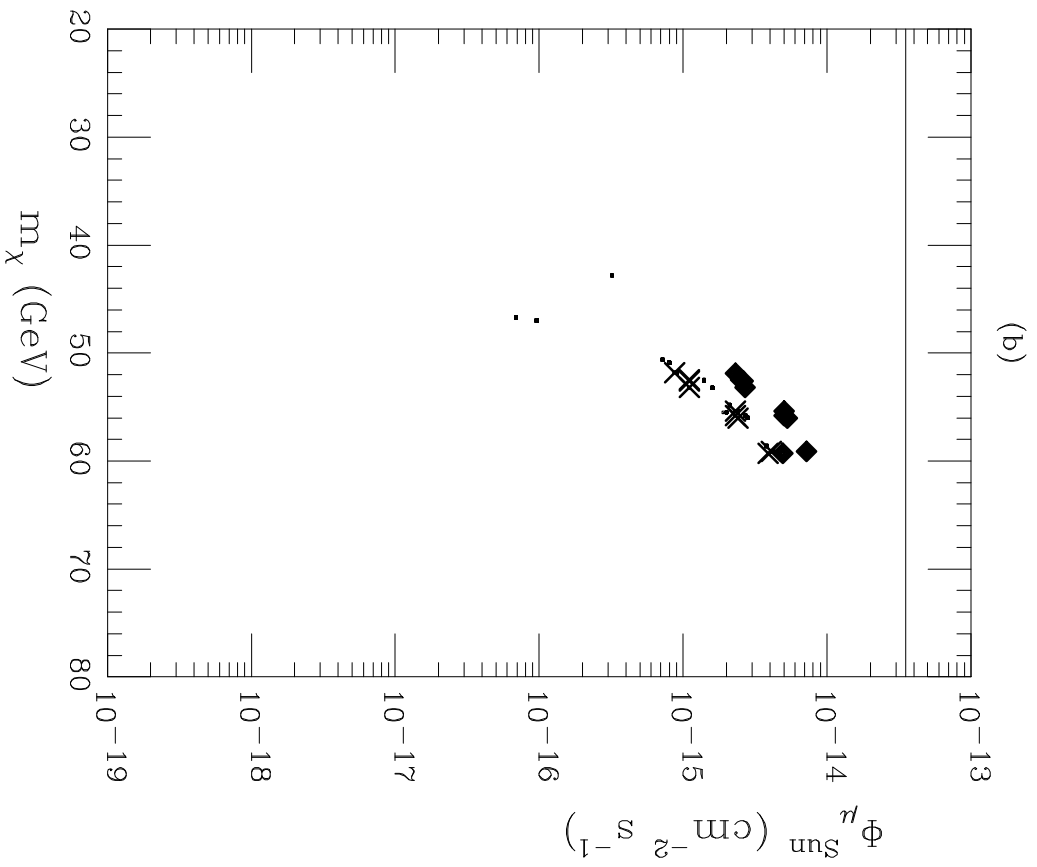
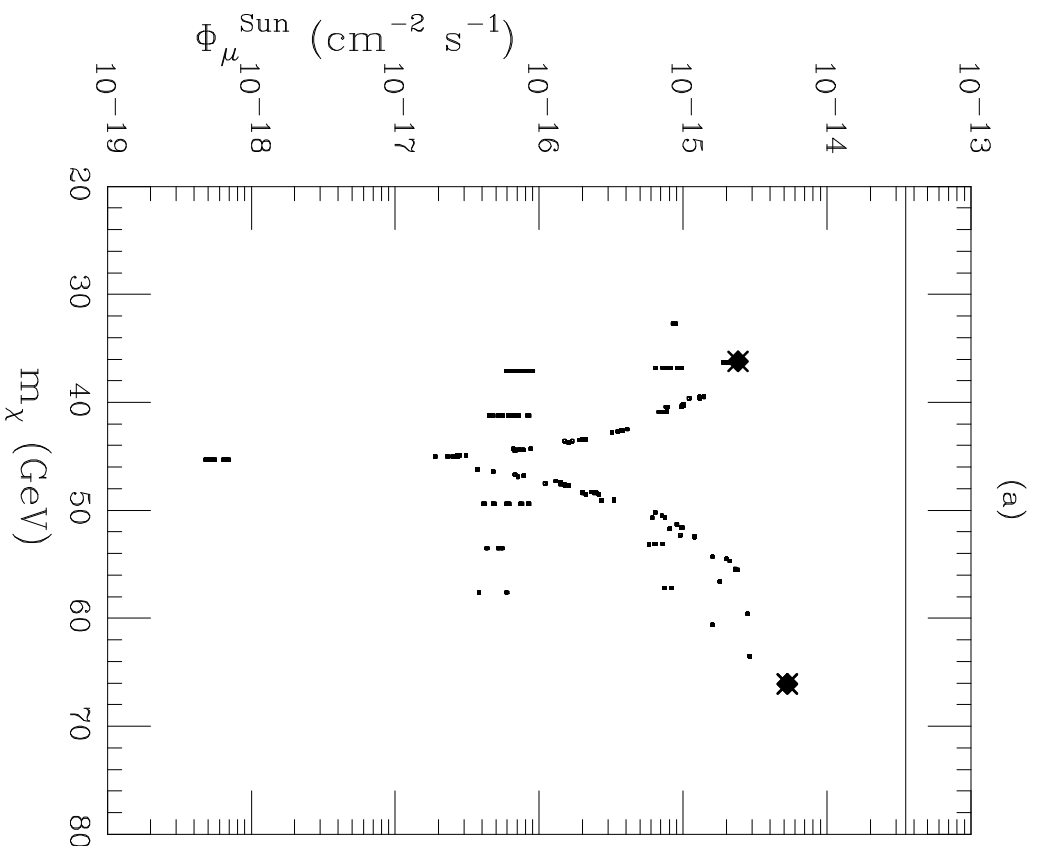


Figure 6

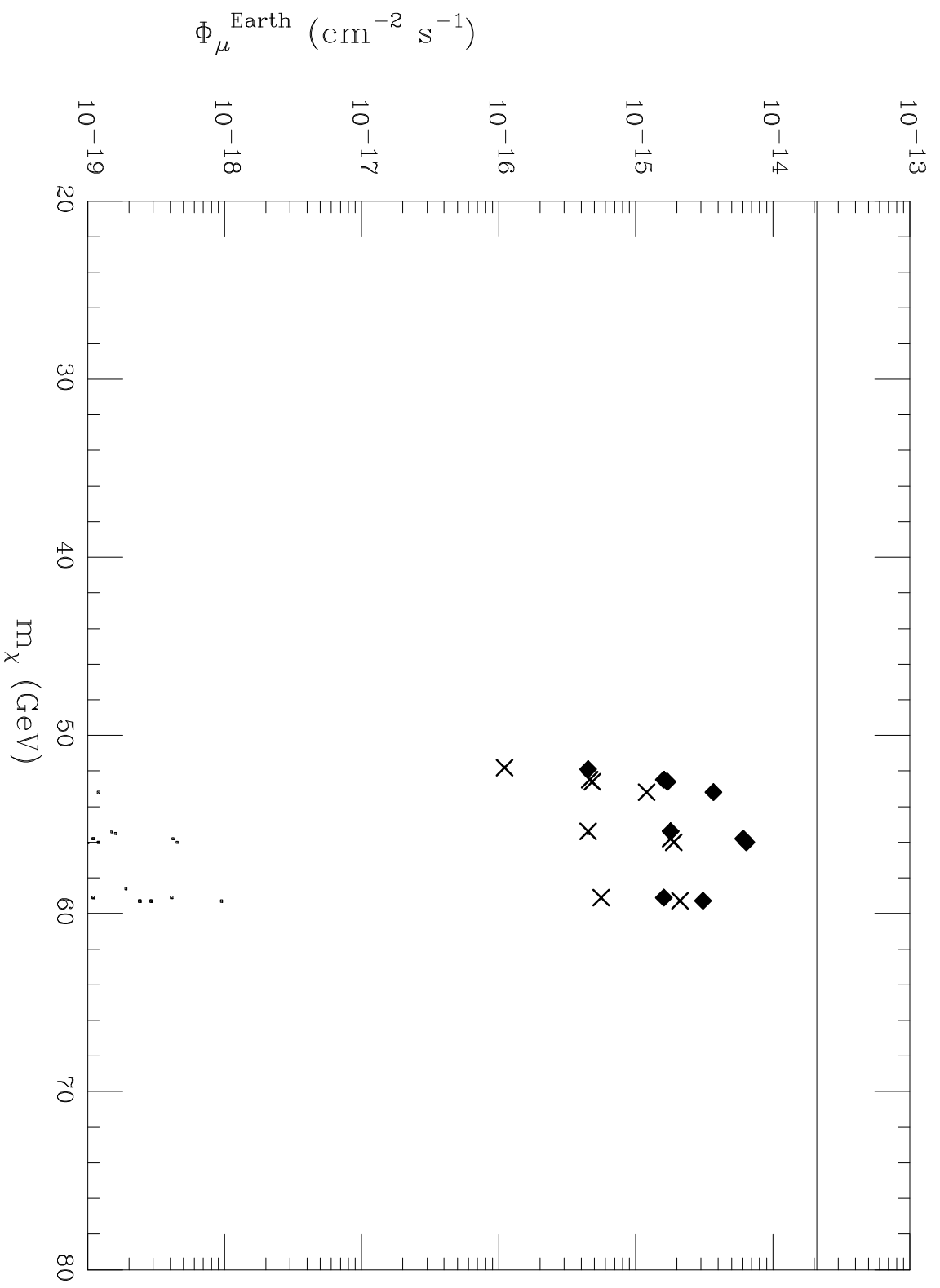


Figure 7

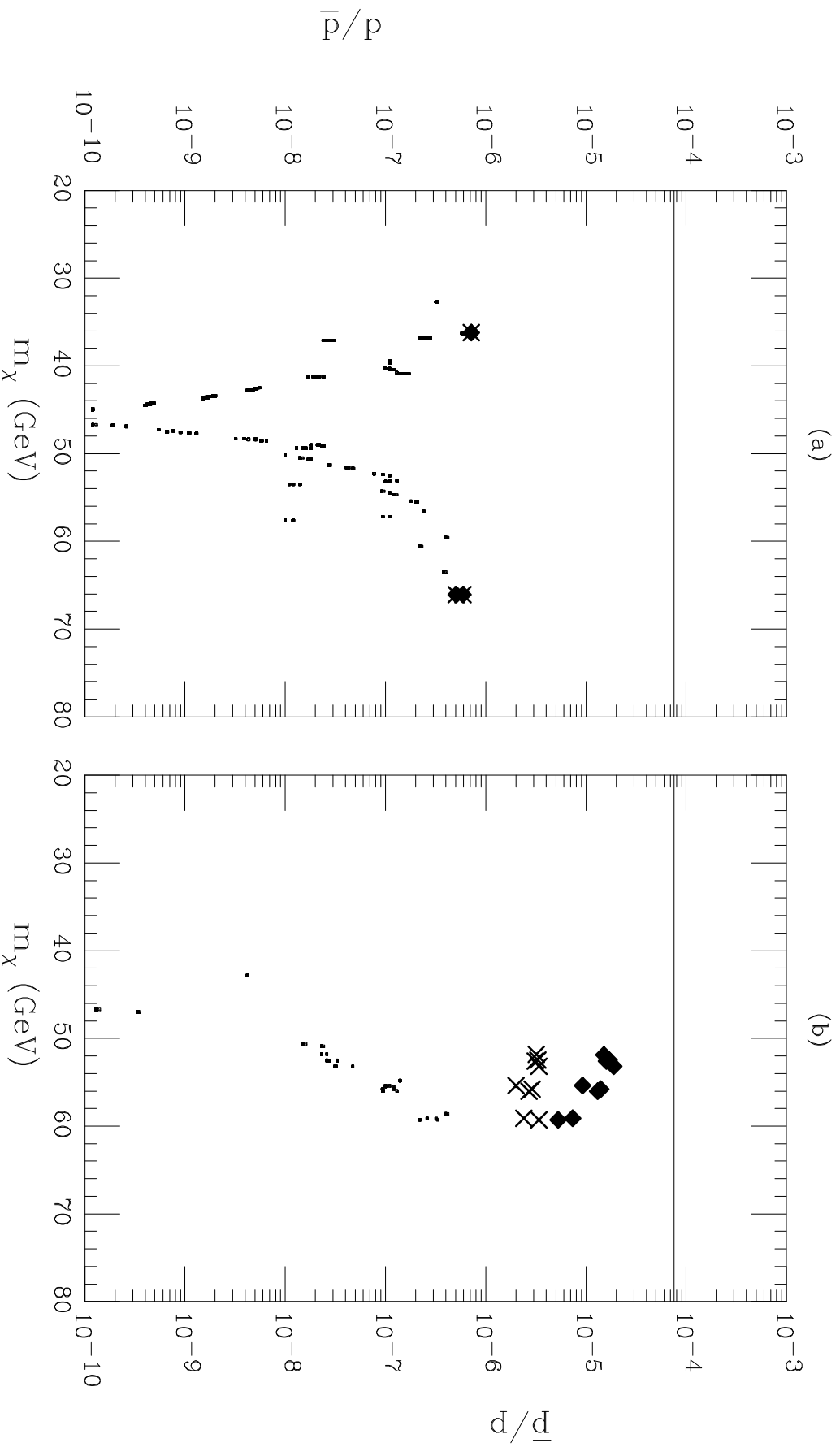


Figure 8



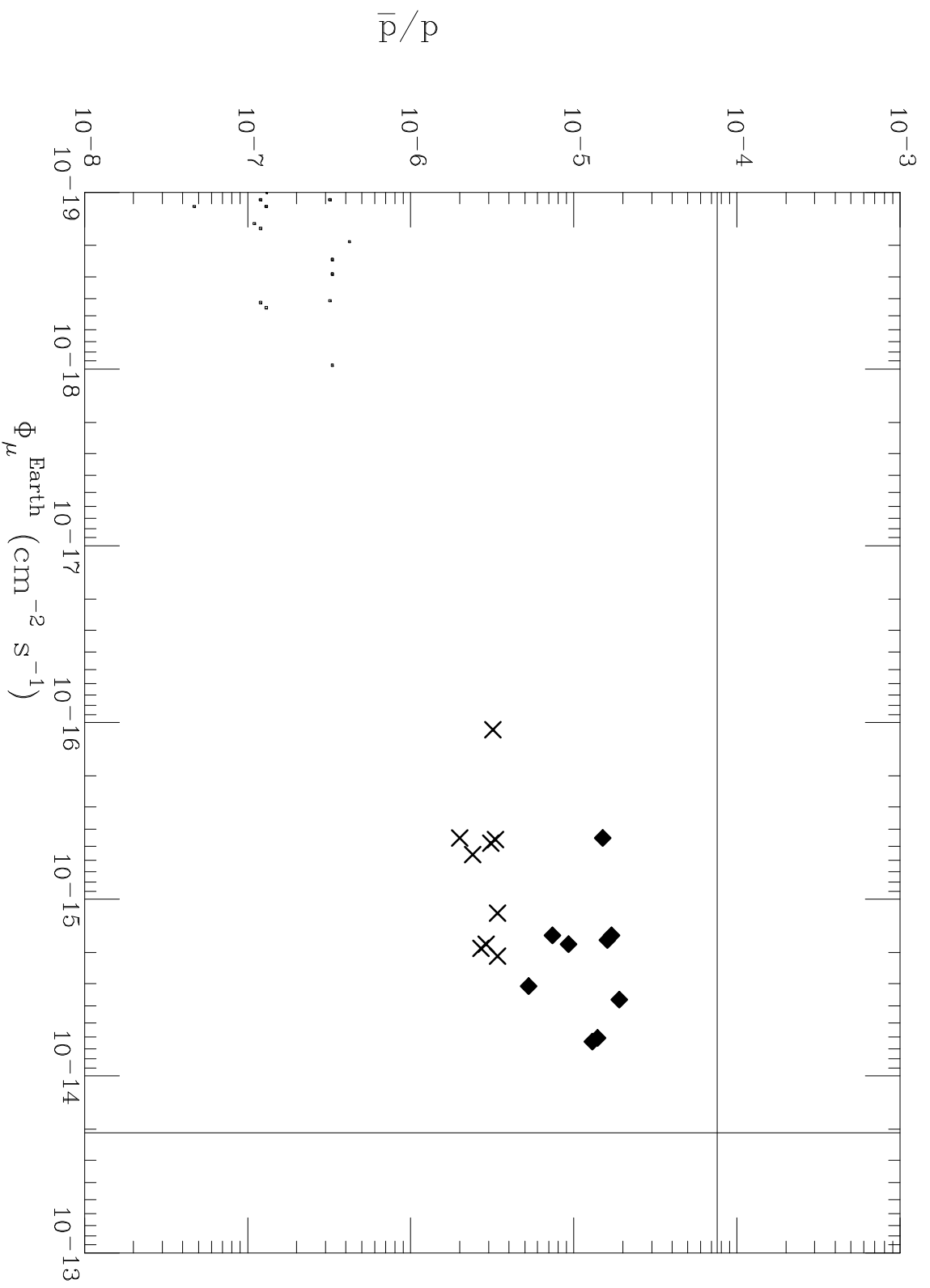


Figure 9

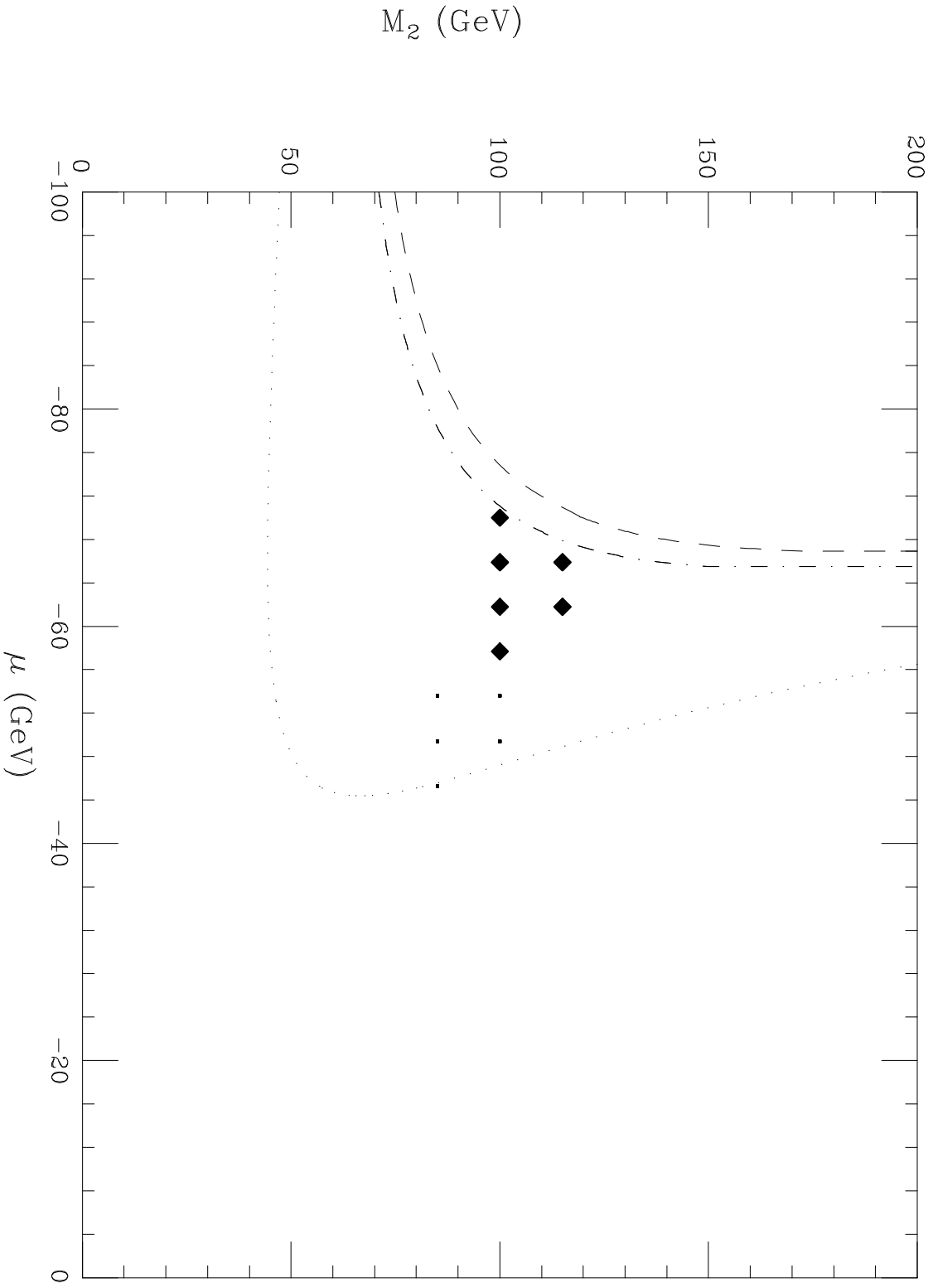


Figure 10